[11]Oskam, B., Bogdonoff, S. M., and Vas, I. E., "Study of Three Dimensional Flow Fields Generated by the Interactions of a Skewed Shock Wave with the Turbulent Boundary Layer," AFFDL-TR-75-21, Feb. 1975.

[12]Horstman, C. C. and Hung, C. M., "Computation of Three Dimensional Turbulent Separated Flows at Supersonic Speeds," AIAA Paper 79-0002, Jan. 1979.

[13]Knight, D. D., "A Hybrid Explicit-Implicit Numerical Algorithm for the Three-Dimensional Compressible Navier-Stokes Equations," AIAA Paper 83-0223, Jan. 1983.

Improved Series Solutions of Falkner-Skan Equation

Noor Afzal*

Aligarh Muslim University, Aligarh, India

Introduction

RECENTLY, Aziz and Na[1] studied a series solution of the Falkner-Skan equation

$$f''' + ff'' + \beta(1 - f'^2) = 0 \tag{1}$$

$$f(0) = f'(0) = 0, \quad f'(\infty) = 1 \tag{2}$$

by expanding the nondimensional stream function f in the powers of β as

$$f = \sum_{n=0}^{\infty} \beta^n f_n(\eta) \tag{3}$$

The lowest order term in Eq. (3) satisfies the Blasius equation

$$f_0''' + f_0 f_0'' = 0 \tag{4}$$

$$f_0(0) = f_0'(0) = 0, \quad f_0'(\infty) = 1 \tag{5}$$

and the higher order perturbations by the recurrence relation

$$f_n''' + f_0 f_n'' + f_0'' f_n = -\delta_{1n} + \sum_{r=1}^{n} f_{r-1}' f_{n-r}' - \sum_{r=1}^{n-1} f_r f_{n-r}'' \tag{6}$$

$$f_n(0) = f_n'(0) = 0, \quad f_n'(\infty) = 0 \tag{7}$$

where δ_{ij} is the well-known Kronecker delta. The first 11 terms in the expansion have been estimated and the result for skin friction is

$$f''(0) = \sum_{n=0} A_n \beta^n \tag{8}$$

where the values of A_n are given in Table 1. For certain specific values of β in the range $-\beta_s < \beta \leq 2$, where

$$\beta_s = 0.198838$$

the results of Eq. (8) were improved by Shanks' transformation. The predictions are in good agreement with exact numerical solutions. However, the range of interest for values of β covers $-\beta_s$ to infinity (see Afzal and Luthra[2] and Evans[3]). Therefore, it is advantageous to improve the convergence of Eq. (8) for a general value of β rather than for the specific values considered by Aziz and Na.[1]

Analysis of the Series

The aim of this Note is to improve the convergence of Eq. (8) by Euler transformation and completing it by determining the remainder. An insight into the location of the nearest singularity can be gained by studying the radius of its convergence (say, β_0), defined by D'Alembert's ratio test

$$\beta_0 = \lim_{n \to \infty} |A_{n-1}/A_n| \tag{9}$$

Domb and Sykes[4] have observed that D'Alembert's limit hopefully can be estimated from a finite number of coefficients by plotting the inverse ratios A_n/A_{n-1} against $1/n$ (known as the Domb-Sykes plot) and extrapolating to $1/n = 0$. The Domb-Sykes plot has the advantage that, for certain common types of functions, the extrapolation turns out to be linear. For example, for the following functions,

$$F = \text{const} \begin{cases} (\beta_0 \pm \beta)^a, & a \neq 0, 1, \ldots \quad (10a) \\ (\beta_0 \pm \beta)^a \log(\beta_0 \pm \beta), & a = 0, 1, \ldots \quad (10b) \end{cases}$$

the inverse coefficients, in the expansion $F = \Sigma A_n \beta^n$,

$$\frac{A_n}{A_{n-1}} = \mp \frac{1}{\beta_0}\left(1 - \frac{1+a}{n}\right) \tag{11}$$

is exactly linear in $1/n$. For more complicated functions the nearest singularity has a leading term similar to Eq. (10) and the ratio A_n/A_{n-1} will behave asymptotically linearly, such as Eq. (11) for large n. The slope of the Domb-Sykes plot gives the nature of the singularity and the inverse of the intercept gives its location.

The Domb-Sykes plot for Eq. (8), shown in Fig. 1, is almost linear. An extrapolation to $1/n$, shown by the line in the figure, leads to the value $1/\beta_0 = 5.03$ or $\beta_0 = 0.1988$, which within the graphical accuracy shows $\beta_0 = \beta_s$. The slope of the line leads to $a = ½$. Therefore, from the Domb-Sykes plot in Fig. 1, we get

$$\beta_0 = \beta_s = 0.198838, \qquad a = ½ \tag{12}$$

Equation (12) shows that Eq. (8) possesses the square root singularity on the real axis in the complex β plane at $\beta = \pm\beta_0$.

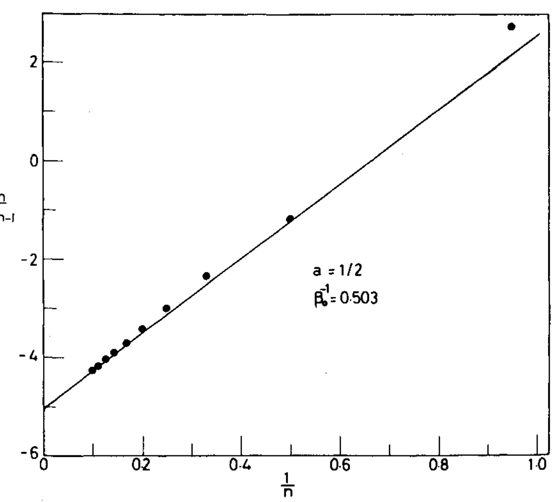

Fig. 1 Domb-Sykes plot for Eq. (8).

Received Oct. 22, 1982.

*Professor, Department of Mechanical Engineering.

For the favorable pressure gradient ($\beta > 0$), the square root singularity is on the negative real axis at $\beta = -\beta_0$; and for the adverse pressure gradient ($\beta < 0$), the square root singularity is on the positive real axis at $\beta = \beta_0$ in the complex β plane. The methods that accelerate the convergence depend on the nature and location of the nearest singularity, therefore, the cases of β positive and negative are treated separately.

For the favorable pressure gradient, the nearest singularity lies off the positive axis. A singularity off the positive axis is of no physical interest, and can be eliminated by mapping it away to infinity by Euler transformation

$$Z = \beta / (\beta + \beta_0) \tag{13}$$

In Eulerizing Eq. (8) we make use of the fact that for strongly accelerated flows $\beta \to \infty$, $f''(0) \sim \beta^{1/2}$ (see Ref. 4). Extracting a factor of $\beta^{1/2}$ and recasting Eq. (8) in terms of the Euler variable Z, we get a new series, which it is hoped is also convergent for strongly accelerated flows,

$$f''(0)\beta^{-1/2} = \sum_{n=0}^{\infty} B_n Z^{n-1/2} \tag{14}$$

where coefficients B_n are given in Table 1.

For the adverse pressure gradient case, the nearest singularity in the complex β plane lies on the positive axis at $\beta = \beta_0$. In general, there is no question of eliminating it short of refining the entire theory. In the present case, however, the square root on the positive axis is an indication that the function is double valued.[5] The dual solutions correspond to the forward and reverse flows in the boundary layer.[6] For the forward flows, Eq. (8) may be improved by extraction of the nearest singularity. As anticipated from Fig. 1, the singularity can be taken proportional to $(\beta_0 + \beta)^{1/2}$. The constant of proportionality is chosen such that the coefficients of the β^{10} term in the two series are equal, which give

$$f''(0) = C_{-1}(1 + \beta/\beta_0)^{1/2} + \sum_{m=0}^{9} C_m \beta^m \tag{15}$$

where coefficients C_m are also given in Table 1. It may be noted that the coefficients of Eq. (15) are greatly reduced and converge much faster than the original series [Eq. (8)].

Table 1 Coefficient of original equation (8), Eulerized equation (14), and completed equation (15)

n	A_n	B_n	C_n
−1	—	—	0.393380
0	0.469600	0.105312E+1	0.076220
0	1.298929	0.526481E−1	0.309733
2	−1.522149	0.230038E−1	−0.278427
3	3.562969	0.117572E−1	0.435495
4	−10.671990	0.644048E−2	−0.841518
5	36.461686	0.364709E−2	1.853965
6	−134.944993	0.208985E−2	−4.407616
7	526.528809	0.119148E−2	10.706481
8	−2132.409912	0.663961E−3	−24.635537
9	8878.316406	0.352970E−3	44.599492
10	−37762.699219	0.171543E−3	—

Table 2 Comparison of the results for $f''(0)$ for moderate pressure gradients

β	Smith[7]	Cebeci and Keller[8]	Aziz and Na[1]	Present[a]
2.0	1.687218	—	1.687516	1.687320
1.6	1.521514	1.521516	1.521689	1.521573
1.2	1.335722	1.335724	1.335793	1.335746
1.0	1.232588	1.232561	1.232623	1.232599
0.8	1.120268	1.120269	1.120280	1.120270
0.6	0.995836	—	0.995837	0.995833
0.4	0.854421	0.854423	0.854418	0.854418
0.2	0.686708	0.686711	0.686706	0.686706
0.1	0.587035	0.587037	0.587034	0.587034
0.05	0.531130	—	0.531129	0.531129
0.0	0.469600	0.469603	0.469600	0.469600
−0.05	0.400323	0.400330	0.400322	0.400322
−0.1	0.319270	0.319278	0.319266	0.319266
0.14	0.239736	—	0.239724	0.239722
−0.16	0.190780	—	0.190758	0.190746
−0.18	0.128636	—	0.128615	0.128504
−0.19	0.085700	0.085702	0.085840	0.085353
−0.195	0.055172	0.055177	0.056027	0.054493

[a] $0 \le \beta \le 2$: Eulerized equation (14); $-\beta_0 < \beta \le 0$: Completed equation (15).

Results

The prediction of numerical results based on Eqs. (14) and (15) is compared here with the available results. The Eulerized equation (14) shows that at $Z = 1(\beta \to \infty)$ the last partial sum of the series yields

$$f''(0)\beta^{-1/2} = 1.155088 \tag{16}$$

whereas the corresponding exact result[2] is 1.154700. For $\beta = 10(5)$, Eq. (14) predicts 3.673610 (2.616217), and when compared with the exact numerical solutions of Evans[3] produces 3.675234 (2.615779). Thus, for large values of β, the present Eulerized series (14) predicts the results with an accuracy of 0.04%. For smaller values of β, the comparison of results from the Eulerized series (14) in the range $0 \le \beta \le 2$ and completed equation (15) for $-\beta_0 < \beta \le 0$ are displayed in Table 2, along with the results of Aziz and Na,[1] Smith,[7] and Cebeci and Keller.[8] Table 2 shows that the present results are correct to four decimal places. Furthermore, most of the values predicted here are slightly better than the predictions of Aziz and Na[1] by Shanks' transformation.

The behavior of Eq. (15) near separation can be explored by introducing a variable $\epsilon = \beta + \beta_0$; $\beta \to -\beta_0$, $\epsilon \to 0$; in Eq. (15) to get

$$f''(0) = \frac{C_{-1}}{\sqrt{\beta_0}}\epsilon^{1/2} + \sum_{n=1}^{\infty} D_n \epsilon^n \tag{17}$$

where constant D_0 ($\simeq -0.0021$) within the numerical accuracy may be regarded as zero. To the leading order, Eq. (17) becomes

$$f''(0) = 0.88219(\beta_0 + \beta)^{1/2}, \qquad \beta \to -\beta_0 \tag{18}$$

This may be compared with the behavior $f''(0) \propto (\beta_0 + \beta)^{1/2}$ anticipated by Brown and Stewartson[6] from the numerical solutions of the Falkner-Skan equation in the neighborhood of separation.

Concluding Remarks

The analysis of Eq. (8) for weak pressure gradients ($\beta \to 0$) yields complete characterization of the solutions. The nature and location of the nearest singularity have been found and the judicious recasting of the series yields very good results even for $\beta \to \infty$. The present analysis also enlightens the singularity in the solutions of Falkner-Skan boundary-layer equation in the neighborhood of separation.

References

[1] Aziz, A. and Na, T. N., "New Approach to the Solutions of Falkner-Skan Equation," *AIAA Journal*, Vol. 19, 1981, pp. 1242-1244.

[2] Afzal, N. and Luthra, V. K., "Highly Accelerated Laminar Flow at Moderately Large Reynolds Numbers," *AIAA Journal*, Vol. 12, 1974, pp. 529-532.

[3]Evans, H. L., *Laminar Boundary-Layer Theory*, Addison-Wesley, London, 1968.

[4]Domb, C. and Sykes, M. E., "On the Susceptibility of a Ferromagnetic Above the Curie Point," *Proceedings of the Royal Society, Ser. A.*, Vol. 240, 1957, pp. 214-228.

[5]Van Dyke, M., "Analysis and Improvement of the Perturbation Series," *Quarterly Journal on Mechanics and Applied Mathematics*, Vol. 27, 1974, pp. 423-450.

[6]Brown, S. N. and Stewartson, K., "Laminar Separation," *Annual Reviews of Fluid Mechanics*, Vol. 1, 1969, p. 50.

[7]Smith, A. M. O., "Improved Solutions of Falkner-Skan Boundary Layer Equations," *Fund Paper, Journal of the Aerospace Sciences*, Sherman M. Fairchild, 1954.

[8]Cebeci, T. and Keller, H. B., "Shooting and Parallel Shooting Methods for Solving Falkner-Skan Equation Boundary Layer Equation," *Journal of Computational Physics*, Vol. 71, 1971, pp. 289-300.

Mean Velocity and Static Pressure Distributions in a Three-Dimensional Turbulent Free Jet

W. R. Quinn*
St. Francis Xavier University, Nova Scotia, Canada
A. Pollard†
Queen's University at Kingston, Ontario, Canada
and
G. F. Marsters‡
Federal Ministry of Transport, Ontario, Canada

Nomenclature

P = static pressure
t_p = height of slot, = 12.7 mm
U = mean streamwise velocity
X, Y, Z = streamwise, spanwise, and lateral coordinates, respectively
ρ = density

Subscripts

ATM = atmospheric value
℄ = value on the jet centerline
EXIT = value of the slot exit plane
LOCAL = local value anywhere within the jet
STAT = static value anywhere within the jet

Introduction

SADDLE-backed velocity distributions are known to exist in turbulent free jet flows from rectangular slots of low or moderate aspect ratio in the plane of the major axis of the respective slots.[1-8] Mean streamwise velocity profiles in such flows are characterized by off-center peaks which are apparently more pronounced in flows from sharp-edged slots.[4-6] Mean streamwise velocity off-center peaks are not found in flows from slots that have smooth contracting upstream shaping in both planes of symmetry.[6]

Some attempts have been made to find an explanation for "saddle-backed" velocity distributions using circumferential[1] streamwise[7] vortex hypotheses. "Turbulence-driven secondary flows" have also been suggested as a possible cause.[9] Vortex stretching hypotheses have been postulated to account for mean streamwise velocity off-center peaks in partially bounded turbulent jet flows from low aspect ratio rectangular slots.[10-12]

The static pressure within the jet might play a role in the formation of these mean streamwise off-center velocity peaks. The present Note provides some mean streamwise velocity and near flowfield static pressure data for the fully three-dimensional turbulent jet flow from a sharp-edged rectangular slot of aspect ratio 10.

Experimental Setup and Procedure

Air, drawn from the laboratory by a small commercial fan supported on antivibration neoprene mounts, was fed into a $0.76 \times 0.61 \times 0.61$ m settling chamber which contained six mesh-wire screens, a baffle, and a filter. The 12.7×127 mm rectangular slot was attached to the downstream face of the settling chamber. The downstream face of the settling chamber was flush with a 2.44×2.44 m plywood wall to ensure tangential entrainment at the slot exit plane. A screen cage ($2.44 \times 2.44 \times 3.66$ m) extending from the wall downstream enclosed the top and sides of the jet and helped to minimize the influence of room draughts, thus facilitating far flowfield measurements. A sketch of the settling chamber, plywood wall, and screen cage is given in Fig. 1. Details of the rectangular slot can be found elsewhere.[13]

Single normal wire and X-wire probes were used for the mean flow measurements. The hot-wire probes were operated by linearized constant temperature anemometers and calibrated in situ in the potential core of the test jet. Air temperature variations of no more than 4°C were monitored with a thermocouple and corrections for this effect and that of

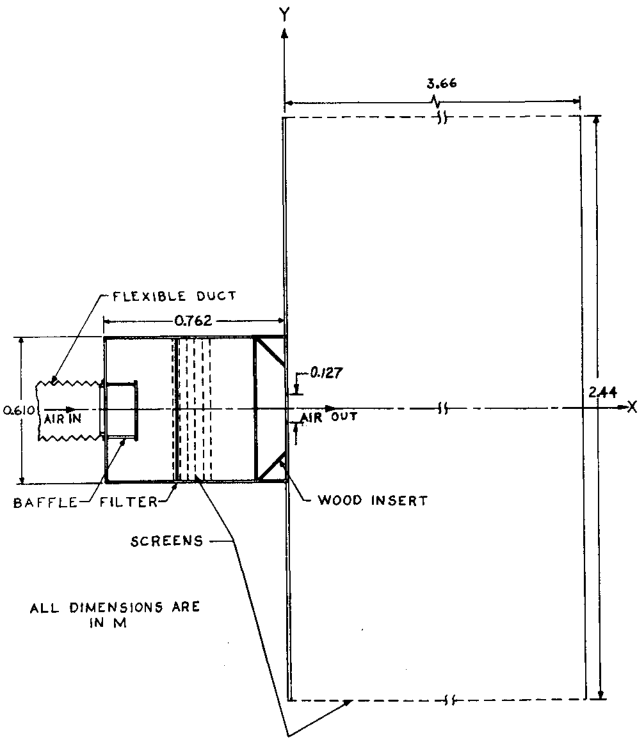

Fig. 1 Top view of settling chamber and screen cage.

Presented as Paper 83-1677 at the AIAA 16th Fluid and Plasma Dynamics Conference, Danvers, Mass., July 12-14, 1983; received Sept. 9, 1983; revision received Aug. 31, 1984.

*Assistant Professor, Department of Engineering. Member AIAA.
†Associate Professor, Department of Mechanical Engineering.
‡Director of Airworthiness. Member AIAA.